Refractometry based on a photonic crystal fiber interferometer

Rajan Jha,[1,*] Joel Villatoro,[1,3] Gonçal Badenes,[1] and Valerio Pruneri[1,2]

[1]*ICFO-Institut de Ciències Fotòniques, Mediterranean Technology Park, 08860 Castelldefels (Barcelona), Spain*
[2]*Also with ICREA-Institució Catalana de Recerca i Estudis Avançats, 08010, Barcelona, Spain*
[3] *joel.villatoro@icfo.es*
**Corresponding author: rajaniitd@gmail.com*

Received December 15, 2008; revised January 21, 2009; accepted January 21, 2009;
posted January 29, 2009 (Doc. ID 105376); published February 24, 2009

We report a simple and compact modal interferometer for applications in refractometry. The device consists of a stub of large-mode-area photonic crystal fiber (PCF) spliced between standard single-mode fibers. In the splice regions the voids of the PCF are fully collapsed, thus allowing the coupling and recombination of PCF core and cladding modes. The device is highly stable over time, has low temperature sensitivity, and is suitable for measuring indices in the 1.330–1.440 range. The measure of the refractive index is carried out by monitoring the shift of the interference pattern. © 2009 Optical Society of America

OCIS codes: 060.2370, 060.5295, 120.3180, 280.4788.

Refractometry is important from both the scientific and technological point of views owing to its numerous applications. On the one hand, the development of simple and compact refractometers is key for applications in industrial processing, quality control in food and beverage industries, etc. Refractive index sensors, on the other hand, are useful for studying different biological or chemical specimens. Optical fiber refractometers and refractive index sensors are attractive, owing to their small size, flexibility in their design, immunity to electromagnetic interference, network compatibility, and the capability for remote and *insitu* measurement. To design a functional optical fiber refractometer one needs to access the evanescent waves of the guided light without compromising the robustness of the device. In addition, an ideal refractometer should be cost effective and able to measure indices over a broad range with high resolution. Refractometers based on tilted Bragg gratings, long-period gratings, and some modal interferometers partially fulfill these conditions, but they suffer from several drawbacks [1–11], such as their high cost and high sensitivity to temperature. Modal interferometers are instead prone to drifts, because they are susceptible to perturbations of the mode coupling conditions.

In this Letter we propose a compact refractometer based on a robust all-fiber modal interferometer fabricated via straightforward and well-established fusion splicing. The device exploits the modal properties of photonic crystal fibers (PCFs), while the interrogation is carried out through pieces of standard optical fibers. The fabrication of the device is simple, since it involves only cleaving and splicing processes that can be carried out in a standard fiber optics lab [12,13]. The range of refractive indices that can be measured is quite broad, from 1.33 (aqueous environments) to 1.44 (biomolecules), with a resolution of $\sim 2.9 \times 10^{-4}$.

Previously reported refractometers and index sensors based on PCF rely on tapering or grating technologies [14–18]. In most of these techniques infiltration of sample into the holes of the PCF is needed. In our case, as it will be clear later, the refractive index measurement is possible through interaction of the evanescent optical field and the material sample in the outer region of the PCF section. To build the device, a few centimeters of commercial PCF (LMA-8 Crystal Fiber A/S) was fusion spliced to a standard optical fiber (Corning SMF-28) with a conventional splicing machine. The splicing was carried out in such a way that the voids of the PCF collapsed completely over a short region, typically less than 300 μm long. Figure 1 shows a micrograph of the PCF employed, a drawing of the interferometer, and a diagram of the experimental setup. To interrogate the interferometer light from a broadband source is launched to the PCF, and the transmitted light is fed to an optical spectrum analyzer. The liquid to be measured is deposited on the PCF outer surface, in a similar way to [19]. However, in the present approach the liquid does not enter the voids of the PCF. Owing to surface tension and intramolecular force, contaminants either in liquid or gas phase can enter open holes of the device in reflection, thus making the cleaning even more difficult, especially for the reusage of the device. In addition, the device in transmission does not require the use of any fiber optic circulator as it was reported in [19]. This not only provides a much broader wavelength operating range

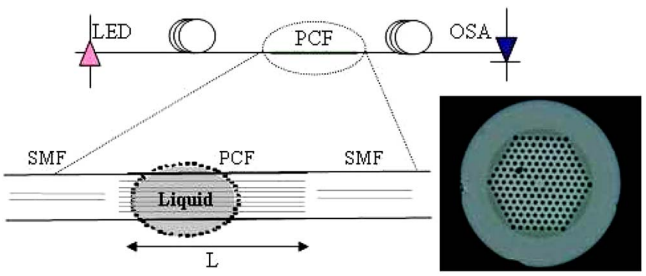

Fig. 1. (Color online) Schematic of the experimental setup, micrograph of the PCF used, and drawing of the interferometer. SMF, single-mode fiber; LED, light-emitting diode; OSA, optical spectrum analyzer; L, length of PCF.

(ten times larger) but also significantly reduces the complexity and cost of the device.

To understand how the interferometer works let us analyze the guided beam when it travels from the SMF to the PCF (Fig. 1). The fundamental SMF mode begins to diffract when it enters a piece of solid glass, i.e., the collapsed PCF region. Because of diffraction the mode broadens allowing the excitation of core and cladding modes in the PCF section [12,13]. The propagation constants of PCF core and cladding modes are different. Thus the modes accumulate a phase difference as they propagate along the PCF section. The phase difference depends on the wavelength of the guided light (λ) and also on the distance over which the modes travel (L, or length of PCF). After the PCF, the modes reach another solid piece of glass, i.e., the other collapsed end of PCF. They will thus further diffract and will be recombined through the filtering of the subsequent SMF. Therefore the transmission of our interferometer can be expressed as that of a two-mode interferometer [8]:

$$T(\lambda) = I_{co}(\lambda) + I_{cl}(\lambda) + 2[I_{co}(\lambda)I_{cl}(\lambda)]^{1/2}\cos(2\pi\Delta n_{ef}L/\lambda), \quad (1)$$

where I_{co} and I_{cl} are the intensities of the core and cladding modes and Δn_{ef} is the difference between the effective refractive indices of core and cladding modes. L is the length of PCF section over which the two modes travel. From Eq. (1) it can be seen that the transmission of our interferometer will exhibit a series of periodic maxima and minima. As an example in Fig. 2, we show the interference pattern over 50 nm of a device fabricated with 80 mm of PCF. The periodic pattern indicates that interference occurs mainly between the fundamental core mode and only one cladding mode. It can be noted that the maxima in these types of interferometers will appear when $2\pi\Delta n_{ef}L/\lambda = 2m\pi$, m being an integer. Therefore the interference pattern exhibits peaks at wavelengths given by $\lambda_m \approx \Delta n_{ef}L/m$. The separation between consecutive peaks (period) is given by $P \approx \lambda^2/\Delta n_{ef}L$.

The performance, stability, and temperature dependence of a modal interferometer depend critically on the element that excites and recombines the modes. In our interferometer the excitation and recombination of modes is carried out with permanent and stable splices. These do not degrade over time or with temperature; thus interferometers with high stability are achievable. In Fig. 2, for example, we show the average drift as a function of time observed in a device fabricated with 80 mm of PCF. We tracked the position of all the peaks over 21 h with a fiber Bragg interrogator with 10 pm resolution. The interferometer was kept straight and isolated during the measurements. Shifts of less than 15 pm were observed indicating the high stability that is important for sensing applications. As it is shown in Fig. 2, the temperature dependence in the range of 24°C–240°C was also studied. Note that for a change in temperature of more than 200°C, the total shift in interference pattern is <1.5 nm, thereby suggesting very low temperature dependence. It was typically in 5–8 pm/°C range depending upon the different device parameters.

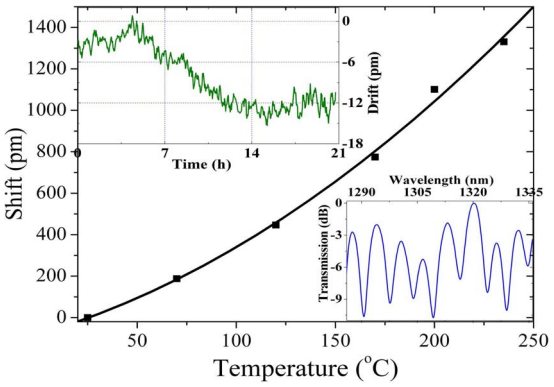

Fig. 2. (Color online) Shift in interference pattern as a function of temperature. Top inset, drift as a function of time observed in 80 mm long interferometer. Bottom inset, interference pattern of the same device over 50 nm in air.

Note that the evanescent waves of cladding modes reach the external surface of the PCF, thus making possible the interaction with liquids or coatings. In our interferometers the interaction is solely with the cladding modes, since the core mode is isolated from the external environment. The interaction of the cladding modes with the external index changes Δn_{ef}, and consequently the phase difference. As a result, the position of the interference peaks and valleys change, or equivalently the interference pattern shifts. Therefore, by monitoring the interference pattern wavelength shift, one can infer the external refractive index and its changes. For example, Figs. 3 and 4 show the transmission spectra in the 1490–1590 nm range of two interferometers, L = 17 mm and 32 mm, respectively, surrounded by air (refractive index of 1) and liquids with higher indices. The shifts observed in both interferometers depended on the external index. The figures also show the shift measured in the 1490–1590 nm wavelength range as a function of the external index in both devices. Deviations from the fitting are justified, since these ex-

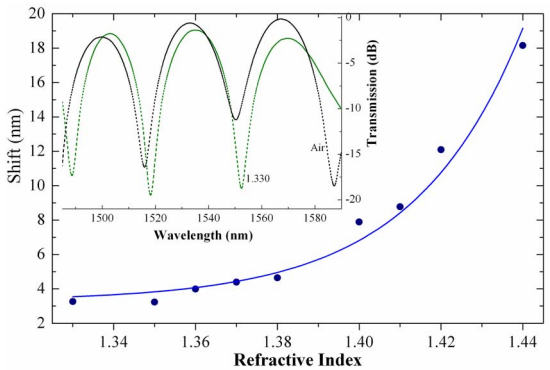

Fig. 3. (Color online) Shift of the interference pattern as a function of the external refractive index observed in a device with L = 17 mm. The solid circles are experimental data, and the continuous curve is a fitting to the data. Shift(nm) = 3.29163 + A[exp(RI/0.02659)] shows the expression that fits to the experimental points with A = 4.75282 $\times 10^{-23}$. Inset, transmission spectra of the device in air and water.

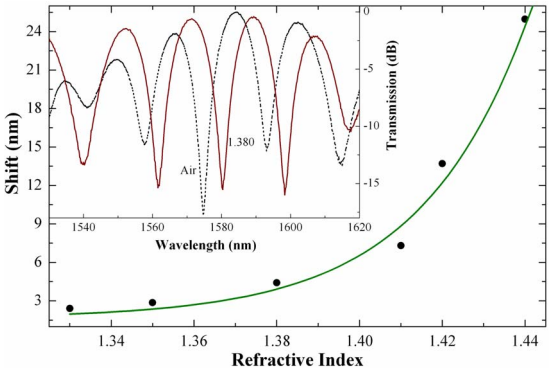

Fig. 4. (Color online) Shift of the interference pattern as a function of the external refractive index observed in a device with $L=32$ mm. The solid circles are experimental data, and the continuous curve is a fitting to the data. Shift(nm)$=2.05046+B[\exp(RI/0.02503)]$ shows the expression that fits to the experimental points with $B=2.3650\times10^{-24}$. Inset, transmission spectra of the device in air and in liquid with an index of 1.380.

perimental points were taken from not perfectly regular interference patterns.

Cargille oils with calibrated indices were used in the experiments. Between consecutive measurements the surface of the PCF was cleaned with acetone and then dried with nitrogen to ensure similar conditions in each measurement. It can be observed from Figs. 3 and 4 that the shift of the interference is more prominent as the external index gets closer to that of the fiber. In this regard our interferometer behaves in a manner similar to those based on gratings [1–8]. Longer devices may be more sensitive owing to a combination of longer interaction lengths and sharper fringes, but shifts of more than one period in a practical situation may be unwelcome. Our devices exhibit maximum sensitivity for indices close to that of the glass of the PCF. Above that value, the cladding mode becomes effectively a radiation mode and the interference pattern disappears. The maximum resolution of the 32-mm-long interferometer in the 1.38–144 index range was found to be $\sim2.9\times10^{-4}$, which is comparable to that of commercial refractometers. However, at indices in the 1.33–1.38 range the resolution is $\sim2\times10^{-3}$. To calculate these numbers it was assumed that a shift of 100 pm can be resolved by the detection unit (although the FBG interrogator that we used has a resolution of 10 pm). It is important to point out that in sensing devices based on shift of fringes, the minimum detectable shift is related with the width (FWHM) of them. In case of broad interference fringes that limit is generally ~FWHM/100. In our case, interferometers with ~10-nm-wide fringes can be fabricated, which justify the above numbers. At shorter wavelengths the resolution is slightly lower in both refractive index ranges. Note that a temperature gradient of approximately 20°C will be required to cause a shift of 100 pm; therefore temperature compensation may not be needed in this type of refractometers if they are used in normal environments.

In conclusion, a compact and simple modal interferometer that operates over a wide wavelength range has been proposed for refractive index measurements. Its fabrication consists of large-mode-area PCF of different lengths spliced between standard single-mode fibers. The refractometric properties of our interferometers were investigated with known liquids in the refractive index range of 1.33–1.45. Sensing based on refractive index changes is also feasible. For example, the PCF can be coated with polymeric, sol gel, or metallic films with literally any index and thickness. Changes in the film refractive index caused by biological, chemical, or physical parameters will cause a detectable shift in the interference pattern.

This work was carried out with the financial support of the Ministerio de Educación y Ciencia (Spain) through grant TEC2006-10665/MIC, "Ramón y Cajal" program, and the European Commission through the European Network of Excellence PHOREMOST (FP6-511616).

References

1. G. Laffont and P. Ferdinand, Meas. Sci. Technol. **12**, 765 (2001).
2. K. Zhou, L. Zhang, X. Chen, and I. Bennion, Opt. Lett. **31**, 1193 (2006).
3. B. H. Lee, Y. Liu, S. B. Lee, S. S. Choi, and J. N. Jang, Opt. Lett. **22**, 1769 (1997).
4. T. Zhu, Y. J. Rao, and Q. J. Mo, IEEE Photon. Technol. Lett. **17**, 2700 (2005).
5. T. Allsop, R. Reeves, D. J. Webb, I. Bennion, and R. Neal, Rev. Sci. Instrum. **73**, 1702 (2002).
6. P. L. Swart, Meas. Sci. Technol. **15**, 1576 (2004).
7. D. W. Kim, Y. Zhang, K. L. Cooper, and A. Wang, Appl. Opt. **44**, 5368 (2005).
8. P. Pilla, P. Foglia Manzillo, M. Giordano, M. L. Korwin-Pawlowski, W. J. Bock, and A. Cusano, Opt. Express **16**, 9765 (2008).
9. Y. Jung, S. Kim, D. Lee, and K. Oh, Meas. Sci. Technol. **17**, 1129 (2006).
10. Q. Wang and G. Farrell, Opt. Lett. **31**, 317 (2006).
11. Z. Tian, S. S. Yam, and H. Loock, Opt. Lett. **33**, 1105 (2008).
12. J. Villatoro, V. P. Minkovich, V. Pruneri, and G. Badenes, Opt. Express **15**, 1491 (2007).
13. J. Villatoro, V. Finazzi, V. P. Minkovich, V. Pruneri, and G. Badenes, Appl. Phys. Lett. **91**, 091109 (2007).
14. V. Minkovich, J. Villatoro, D. Monzon-Hernandez, S. Calixto, A. Sotsky, and L. Sotskaya, Opt. Express **13**, 7609 (2005).
15. M. C. P. Huy, G. Laffont, V. Dewynter, P. Ferdinand, L. Labonte, D. Pagnoux, P. Roy, W. Blanc, and B. Dussardier, Opt. Express **14**, 10359 (2006).
16. Y. Zhu, Z. He, and H. Du, Sens. Actuators B **131**, 265 (2008).
17. L. Rindorf and O. Bang, Opt. Lett. **33**, 563 (2008).
18. C. Chen, A. Laronche, G. Bouwmans, L. Bigot, Y. Quiquempois, and J. Albert, Opt. Express **16**, 9645 (2008).
19. R. Jha, J. Villatoro, and G. Badenes, Appl. Phys. Lett. **93**, 191106 (2008).